

# An Improved Reversible Data Hiding in Encrypted Images Using Parametric Binary Tree Labeling

Youqing Wu<sup>ID</sup>, Youzhi Xiang<sup>ID</sup>, Yutang Guo, Jin Tang, and Zhaoxia Yin<sup>ID</sup>, Member, IEEE

**Abstract**—This work proposes an improved reversible data hiding scheme in encrypted images using parametric binary tree labeling(IPBTL-RDHEI), which takes advantage of the spatial correlation in the entire original image but not in small image blocks to reserve room for hiding data. Then the original image is encrypted with an encryption key and the parametric binary tree is used to label encrypted pixels into two different categories. Finally, one of the two categories of encrypted pixels can embed secret information by bit replacement. According to the experimental results, compared with several state-of-the-art methods, the proposed IPBTL-RDHEI method achieves higher embedding rate and outperforms the competitors. Due to the reversibility of IPBTL-RDHEI, the original plaintext image and the secret information can be restored and extracted losslessly and separately.

**Index Terms**—Image encryption, reversible data hiding, parametric binary tree labeling, separately.

## I. INTRODUCTION

REVERSIBLE data hiding (RDH) in the plaintext domain is a technique to modify the original cover image to hide secret information (secret data) [1]–[4]. It can completely restore the original cover image after extracting the secret information. In the last decade, reversible data hiding has attracted extensive research interest from the information hiding community, due to its potential applications when images are not allowed to be disturbed. As of now, many methods have been designed, which can be mainly classified into three different categories: lossless compression-based [5], [6], difference expansion-based [7]–[9] and histogram shifting-based [10], [11] methods. These methods

Manuscript received June 10, 2019; revised September 27, 2019; accepted November 2, 2019. Date of publication November 11, 2019; date of current version July 24, 2020. This work was supported in part by the National Natural Science Foundation of China under Grants 61872003, U1636206, 61872005, and 61860206004 and in part by the Natural Science Foundation of Anhui Higher Education Institutions of China under Grant KJ2013A217. The associate editor coordinating the review of this manuscript and approving it for publication was Prof. Abdulmotaleb El Saddik. (*Corresponding author:* Zhaoxia Yin.)

Y. Wu is with the School of Key Laboratory of Intelligent Computing and Signal Processing, Ministry of Education, Anhui University, Hefei 230601, China, and also with the School of Computer Science and Technology, Hefei Normal University, Hefei 230601, China (e-mail: wuyq.hfnu@qq.com).

Y. Xiang, J. Tang, and Z. Yin are with the School of Key Laboratory of Intelligent Computing and Signal Processing, Ministry of Education, Anhui University, Hefei 230601, P. R. China (e-mail: 1875738190@qq.com; tj@ahu.edu.cn; yinzhaoxia@ahu.edu.cn).

Y. Guo is with the School of Computer Science and Technology, Hefei Normal University, Hefei 230601, P. R. China (e-mail: guoyutang@hfnu.edu.cn).

Color versions of one or more of the figures in this article are available online at <http://ieeexplore.ieee.org>.

Digital Object Identifier 10.1109/TMM.2019.2952979

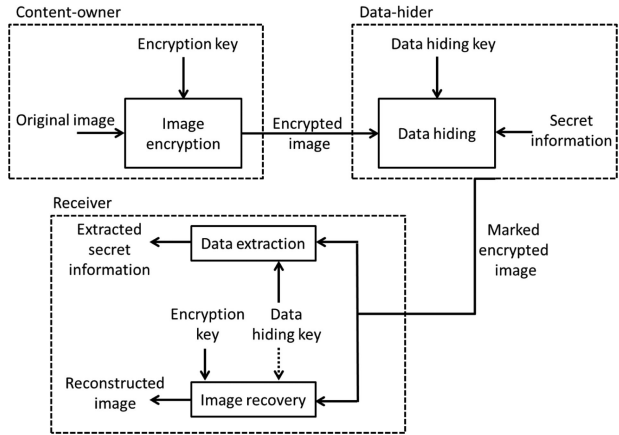


Fig. 1. The framework of RDHEI methods.

aim to ensure the secret information cannot be detected and the change of the cover image is not perceptible.

With the increasing demand for user privacy protection on cloud storage, many reversible data hiding schemes in encrypted images (RDHEI) have been published since the pioneering work proposed by Puech [12]. The RDHEI technology embeds secret information into encrypted images rather than plaintext images [13]–[16], which involves three parties: the content-owner, data-hider, and receiver. The original image provider (the content-owner) encrypts the original image before sending it to the cloud. The cloud manager (the data-hider) embeds secret information into encrypted image without knowing the original plaintext image or encryption key. For the receiver, the original plaintext image can be restored and the secret information can be extracted. Fig. 1 shows the framework of RDHEI methods precisely.

In general, the reported RDHEI techniques can be mainly classified into three different categories, 1) vacating room after encryption (VRAE) [13], [17]; 2) vacating room by encryption (VRBE) [18]; and 3) reserving room before encryption (RRBE) [19]–[21]. Since encryption operation disrupts the spatial correlation of the original plaintext image, thus it is difficult for VRAE methods to achieve satisfactory embedding capacity. The VRBE methods use some special encryption schemes to encrypt the original plaintext image while keeping partly spatial correlation in the image after encryption. Since the spatial redundancy is not fully utilized in VRBE methods, thus the embedding capacity is also limited. Different from VRBE and VRAE, the RRBE methods have been proposed to exploit spatial correlation

in the original plaintext image, which reserve room before image encryption so as to obtain higher embedding capacity.

In the previous RDHEI methods, image-recovery and secret information extraction should be processed jointly [13]. To separate the process of image-recovery and secret information extraction, separable RDH in the encryption domain have been studied [17]–[21]. Zhang [17] proposed a separable RDHEI scheme to free up a sparse space to accommodate secret information by compressing the least significant bits. Yi *et al.* [18] proposed a VRBE separable RDHEI method using parametric binary tree labeling to embed secret information by exploiting local correlation within small image blocks. Puteaux *et al.* [19] proposed to use MSB substitution to embed secret information. Due to the spatial correlation in a plaintext image, the original image can be restored based on MSB prediction and the secret information can be extracted from the MSB plane. But the method in [19] only substitutes one-MSB for embedding secret information, thus the embedding rate is lower than one bit per pixel (bpp). Based on [19], an improved method proposed in [20] to embed secret information by two-MSB (MSB and second MSB) planes substitution so that the embedding rate can exceed 1 bpp. Chen *et al.* [21] transformed the block-based MSB planes of the original plaintext image into bits stream and adopted run-length coding to compress the bits stream for embedding secret information, but the embedding rate is also not very ideal.

Since Yi *et al.* [18] only used the redundancy in small image blocks but not in the entire image, thus the spatial redundancy is not fully utilized. Based on Yi *et al.*'s method [18], an improved reversible data hiding scheme in encrypted images using parametric binary tree labeling (PBTL-RDHEI) is proposed in this paper, which is a high capacity RRBE separable RDHEI method. First, the content-owner reserves embedding room in the plaintext image before encryption and uses a parametric binary tree to label encrypted pixels into two different categories for hiding secret information. Second, the data-hider embeds secret information into one of the two categories of encrypted pixels by bit replacement. Third, according to different permissions, the receiver can obtain the original plaintext image, secret information or both. Compared with Yi *et al.*'s method [18], the proposed PBTL-RDHEI method takes full advantage of the image redundancy and achieves a higher embedding rate.

The main contributions of this paper are as follows:

- 1) The proposed PBTL-RDHEI method reserves room in the plaintext image before encryption, which takes full advantage of the spatial correlation in the entire original image but not in small image blocks for embedding data.
- 2) We present an effective method of RDH in the encryption domain using parametric binary tree labeling and obtain higher embedding rate than state-of-the-art methods. The proposed PBTL-RDHEI method is separable and error-free in image-recovery and data-extraction.

The rest of this paper is structured as follows. Section II introduces parametric binary tree labeling scheme. The proposed PBTL-RDHEI method is elaborated in Section III. Section IV shows the experimental results and analysis. Section V concludes this paper with prospective future works.

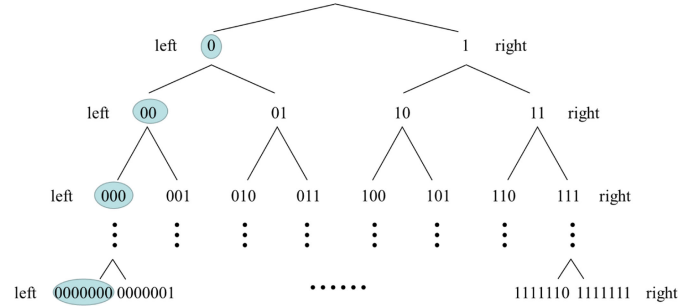


Fig. 2. The distribution of binary codes in a full binary tree.

TABLE I  
ILLUSTRATIVE EXAMPLE OF LABELING BITS SELECTION WHEN  $\beta = 1$  AND  $\alpha = 1$  TO 7

$\beta = 1$	G2	G1	$n_\alpha$
$\alpha = 1$	0	1	1
$\alpha = 2$	0	11, 10	2
$\alpha = 3$	0	111, 110, 101, 100	4
$\alpha = 4$	0	1111 ~1000	8
$\alpha = 5$	0	11111 ~10000	16
$\alpha = 6$	0	111111 ~100000	32
$\alpha = 7$	0	1111111 ~1000000	64

## II. PARAMETRIC BINARY TREE LABELING SCHEME

The pixels in an image can be separated into two different categories by parametric binary tree labeling scheme (PBTL) [18]. Fig. 2 is a full binary tree that is used to illustrate the distribution of binary codes.

For image pixels with 8-bit depth, the full binary tree has 7 layers, and the  $i^{\text{th}}$  layer has  $2^i$  nodes, where  $i = 1, 2, \dots, 7$ . Given two parameters  $\alpha$  and  $\beta$ , where  $1 \leq \alpha, \beta \leq 7$ , the pixels in two different categories assumed as G1 and G2 are labeled as follows. For G2, all pixels are labeled by the same  $\beta$ -bit of '0...0', which is the first node of the  $\beta^{\text{th}}$  layer. For G1, all pixels are classified into  $n_\alpha$  different sub-categories, and we use the following Eq. (1) to calculate the positive integer  $n_\alpha$  [18]:

$$n_\alpha = \begin{cases} 2^\alpha - 1, & \alpha \leq \beta \\ (2^\beta - 1) * 2^{\alpha-\beta}, & \alpha > \beta \end{cases} \quad (1)$$

When  $\alpha \leq \beta$ , the  $2^\alpha - 1$  nodes from right to left in the  $\alpha^{\text{th}}$  layer are selected to label  $n_\alpha$  different sub-categories in G1. When  $\alpha > \beta$ , the  $(2^\beta - 1) * 2^{\alpha-\beta}$  nodes from right to left in the  $\alpha^{\text{th}}$  layer are selected to label  $n_\alpha$  different sub-categories in G1, that is, when  $\alpha > \beta$ , the selected  $n_\alpha$  binary nodes that are not derived from the first node of the  $\beta^{\text{th}}$  layer of '0...0'. Moreover, pixels in the same sub-category are labeled with the same  $\alpha$ -bit binary code, and pixels in different sub-categories are labeled with different  $\alpha$ -bit binary codes. Table I and Table II

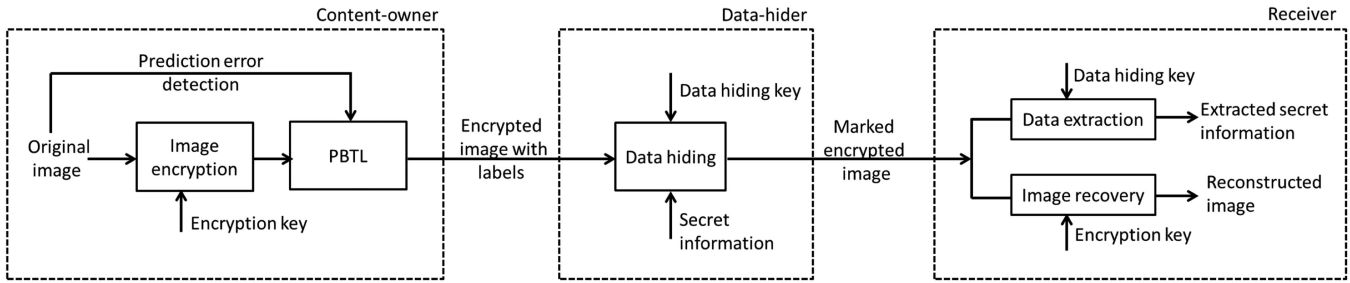


Fig. 3. The framework of the proposed IPBTL-RDHEI method.

TABLE II  
ILLUSTRATIVE EXAMPLE OF LABELING BITS SELECTION WHEN  $\beta = 2$  AND  $\alpha = 1$  TO 7

$\beta = 2$	G2	G1	$n_\alpha$
$\alpha = 1$	00	1	1
$\alpha = 2$	00	11, 10, 01	3
$\alpha = 3$	00	111, 110, 101, 100, 011, 010	6
$\alpha = 4$	00	1111 ~0100	12
$\alpha = 5$	00	11111 ~01000	24
$\alpha = 6$	00	111111 ~010000	48
$\alpha = 7$	00	1111111 ~0100000	96

are two illustrative examples of labeling bits selection when  $\beta = 1$  to 2 and  $\alpha = 1$  to 7.

As can be seen from Tables I-II, for example, when  $\alpha = 3$ ,  $\beta = 2$ , all the pixels in G2 are labeled by ‘00,’ and the  $(2^\beta - 1) * 2^{\alpha-\beta} = 6$  nodes from right to left in the 3<sup>th</sup> layer are selected to label 6 different sub-categories in G1. The 6 selected nodes are ‘111,’ ‘110,’ ‘101,’ ‘100,’ ‘011’ and ‘010,’ which are not derived from the node of ‘00,’ that is, ‘000’ and ‘001’ that derived from ‘00’ are ignored and the remaining nodes in the 3<sup>th</sup> layer are kept.

### III. PROPOSED SCHEME

The proposed IPBTL-RDHEI method is composed of three main phases: 1) Generation of encrypted image with labels done by the content-owner, 2) Generation of marked encrypted image done by the data-hider, and 3) Data-extraction/image-recovery done by the receiver. In the first phase, the content-owner detects the prediction errors of the original plaintext image and encrypts the original plaintext image using the encryption key. Then, PBTL is used to label encrypted pixels into embeddable pixel set and non-embeddable pixel set. In the second phase, after using the data-hiding key, the secret information can be hidden by bit replacement in embeddable pixel set. In the third phase, the secret information must be extracted without error from the marked encrypted image with only the data-hiding key, and the original plaintext image must be reconstructed losslessly by exploiting the spatial correlation with only the encryption key. When using both of the keys, the original plaintext image and

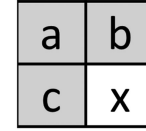


Fig. 4. The context of the MED predictor.

the secret information must be restored and extracted losslessly. Fig. 3 illustrates the framework of the proposed IPBTL-RDHEI method.

#### A. Generation of Encrypted Image With labels

This stage has four steps: prediction error detection, image encryption, pixel grouping and pixel labeling using PBTL, which are introduced below:

1) *Prediction Error Detection:* For an original plaintext image, the pixels on the first row and first column are retained as reference pixels. The median edge detector (MED) predictor [8] shown in Fig. 4 can exploit the left, upper and upper left neighboring pixels to predict an image pixel:

$$px = \begin{cases} \max(b, c), & a \leqslant \min(b, c) \\ \min(b, c), & a \geqslant \max(b, c) \\ b + c - a, & \text{otherwise} \end{cases} \quad (2)$$

where  $px$  is the prediction value of  $x$ . Hence the prediction error  $e$  is calculated by:

$$e = x - px \quad (3)$$

2) *Image Encryption:* After obtaining all the prediction errors of the 8-bit depth original image  $I$ , we convert each pixel in the original image  $I$  into 8-bit binary sequence using:

$$x^k(i, j) = \lfloor x(i, j)/2^{k-1} \rfloor \bmod 2, \quad k = 1, 2, \dots, 8 \quad (4)$$

where  $k$  is the corresponding bit of the binary sequence,  $1 \leqslant i \leqslant m$  and  $1 \leqslant j \leqslant n$ ,  $m * n$  is the size of the original image  $I$  and  $\lfloor \cdot \rfloor$  is floor operation. A pseudo-random matrix  $R$  of the same size as the original image  $I$  is generated by an encryption key. Similarly, each pixel  $r(i, j)$  in  $R$  is converted into 8-bit binary sequence using Eq. (4). Then the encrypted 8-bit binary sequence can be obtained by the bitwise exclusive-or (XOR) operation:

$$x_e^k(i, j) = x^k(i, j) \oplus r^k(i, j), \quad k = 1, 2, \dots, 8 \quad (5)$$

152	153	152	152	153
149	152	151	147	155
153	151	151	149	153
151	154	153	150	147

152	153	152	152	153
149	150	152	151	148
153	153	151	147	155
151	151	154	151	153

x	x	x	x	x
x	2	-1	-4	7
x	-2	0	2	-2
x	3	-1	-1	-6

27	246	198	189	235
224	45	158	36	25
192	137	166	60	30
143	142	225	248	1

Fig. 5. Example of prediction error detection and image encryption: (a) original image, (b) prediction values, (c) prediction errors and (d) encrypted image.

where  $\oplus$  is the bitwise XOR operation, and  $x_e^k(i, j)$  denotes the encrypted 8-bit binary sequence. Finally, Eq. (6) is used to calculate the encrypted pixel  $x_e(i, j)$ :

$$x_e(i, j) = \sum_{k=1}^8 x_e^k(i, j) \times 2^{k-1}, \quad k = 1, 2, \dots, 8 \quad (6)$$

In this way, the encrypted image  $I_e$  is generated. Fig. 5 shows an example of prediction error detection and image encryption. Fig. 5(a) is taken as the original image, where  $m = 4$  and  $n = 5$ . The corresponding prediction values of Fig. 5(a) are shown in Fig. 5(b), the pixels on the first row and first column are retained as reference pixels. Fig. 5(c) shows the prediction errors from the subtraction of Fig. 5(a) and Fig. 5(b). Without loss of generality, Fig. 5(d) is assumed to be an encrypted image of Fig. 5(a) by an encryption key  $k_e$ .

**3) Pixel Grouping:** We separate all the pixels in encrypted image  $I_e$  into reference pixel set ( $P_r$ ), special pixel set ( $P_s$ ), embeddable pixel set ( $P_e$ ) and non-embeddable pixel set ( $P_n$ ). The pixels on the first row and first column belong to  $P_r$ , which will be kept unchanged during the generation of marked encrypted image. We can pick any one pixel to be  $P_s$ , which will be used to store the parameters  $\alpha$  and  $\beta$ . Then, for each remaining pixel  $I_{e_i}$  ( $i = 1, 2, \dots, m * n - (m + n - 1) - 1$ ), according to the corresponding prediction error  $e_i$  ( $i = 1, 2, \dots, m * n - (m + n - 1) - 1$ ) calculated by Eq. (3), if  $e_i$  meets the condition of Eq. (7) [18], the pixel  $I_{e_i}$  belongs to  $P_e$ ; otherwise, it belongs to  $P_n$ . Pixels in  $P_e$  can embed secret information while  $P_n$  cannot.

$$\left\lceil -\frac{n_\alpha}{2} \right\rceil \leq e_i \leq \left\lfloor \frac{n_\alpha - 1}{2} \right\rfloor \quad (7)$$

where  $n_\alpha$  is calculated by Eq. (1),  $\lceil \cdot \rceil$  is the ceil operation and  $\lfloor \cdot \rfloor$  is the floor operation. Let  $n_r$ ,  $n_e$  and  $n_n$  represent the number of pixels in  $P_r$ ,  $P_e$  and  $P_n$ , respectively. Thus,  $m * n = n_r + n_e + n_n + 1$ , and  $n_r = m + n - 1$ .

Fig. 6 is the pixel grouping of Fig. 5 when  $\alpha = 3$  and  $\beta = 2$ . According to aforementioned, we pick pixels on first row and column as  $P_r$ . Without loss of generality, the last pixel is selected as  $P_s$ . By the Eq. (1) and Eq. (7), if the prediction error  $e_i$  meets the condition:  $-3 \leq e_i \leq 2$ , the pixel  $I_{e_i}$  belongs to  $P_e$ ; otherwise, it belongs to  $P_n$ .

**4) Pixel Labeling using PBTL:** Since the positions of  $P_r$  and  $P_s$  are predefined, we just need to label the pixels in  $P_e$  and  $P_n$  using the PBTL scheme. Given two parameters  $\alpha$  and  $\beta$ , all the pixels in  $P_n$  are labeled by the same  $\beta$ -bit of ‘0...0’, and the remaining  $(8 - \beta)$ -bit of each pixel should be kept unchanged. For  $P_e$ , all pixels are classified into  $n_\alpha$  different sub-categories according to different prediction errors. Moreover, pixels in the same sub-category are labeled with the same  $\alpha$ -bit binary code, and pixels in different sub-categories are labeled with different  $\alpha$ -bit binary codes. Note that due to the spatial correlation of the original image, the prediction errors of the adjacent pixels are likely to be the same, and then the adjacent pixels are likely to be labeled with the same binary code. If the most significant bits of each pixel are used to be labeled by bit replacement, which may reveal the original image content. To avoid this issue, the least significant bits of each pixel are adopted instead of the most significant bits for labeling, that is, for  $P_e$  and  $P_n$ , we arrange the 8-bit binary sequence of each pixel in reverse order before pixel labeling using PBTL.

### B. Generation of Marked Encrypted Image

The parameters  $\alpha$  and  $\beta$  are first stored in  $P_s$ . Since  $1 \leq \alpha, \beta \leq 7$ ,  $P_s$  is sufficient to store them by bit replacement, then the original 8-bit of  $P_s$  is stored as auxiliary information. In addition, for all the pixels in  $P_n$ , the replaced original  $\beta$ -bit of each pixel need to be recorded as auxiliary information. Thus, the auxiliary information contains two parts: the original 8-bit of  $P_s$  and the replaced original  $\beta$ -bit of each pixel in  $P_n$ . The payload consists of auxiliary information and secret information.

Each pixel in  $P_e$  is labeled with  $\alpha$ -bit binary code during pixel labeling, then the remaining  $(8 - \alpha)$ -bit is reserved for hiding payload bits by bit replacement. Therefore, the data-hider can successfully embed the payload of  $(8 - \alpha) * n_e$  bits, including auxiliary information of  $8 + \beta * n_n$  bits and secret information of  $(8 - \alpha) * n_e - (8 + \beta * n_n)$  bits. For data security, the secret information is first encrypted by using the data hiding key  $k_d$  before the embedding operation. In this way, the marked encrypted image is generated.

Given different parameters  $\alpha$  and  $\beta$ , the net embedding rate  $r_{\alpha, \beta}$  (bpp) [18] can be calculated as:

$$r_{\alpha, \beta} = \frac{(8 - \alpha) * n_e - (8 + \beta * n_n)}{m * n} \quad (8)$$

In practice, we further obtain the maximum net embedding rate  $r_{\max}$  (bpp) [18] as:

$$r_{\max} = \max(r_{\alpha, \beta})_{\alpha=1, \beta=1}^7 \quad (9)$$

Fig. 7 shows an example of pixel labeling and payload embedding when  $\alpha = 3$  and  $\beta = 2$ . Fig. 7(a) indicates the labeling bits selection of  $P_e$  and  $P_n$ . Here, ‘00’ is used to label each pixel in  $P_n$ , ‘111’, ‘110’, ‘101’, ‘100’, ‘011’ and ‘010’ are used to label

$P_r$	$P_r$	$P_r$	$P_r$	$P_r$
$P_r$	$P_e$	$P_e$	$P_n$	$P_n$
$P_r$	$P_e$	$P_e$	$P_e$	$P_e$
$P_r$	$P_n$	$P_e$	$P_e$	$P_s$

Fig. 6. Pixel grouping.

pixels in  $P_e$  when the prediction error equal to 2, 1, 0,  $-1$ ,  $-2$  and  $-3$ , respectively. Fig. 7(b) represents the 8-bit binary sequence of Fig. 5(d). Fig. 7(c) denotes the reverse order of each pixel in  $P_e$  and  $P_n$ . Fig. 7(d) shows pixel bits after pixel labeling. Fig. 7(e) is the encrypted image with labels and Fig. 7(f) is the marked encrypted image after payload embedding. As can be seen, the pixels in  $P_r$  remain unchanged, then the first 4 bits of  $P_s$  are utilized to store  $\alpha$  and the last 4 bits of  $P_s$  are utilized to store  $\beta$ . Each pixel in  $P_n$  is labeled with ‘00’ and each pixel in  $P_e$  is labeled with 3-bit binary code according to different prediction error. The ‘-----’ in Fig. 7(f) represents the bits that have been embedded payload. Note that the payload contains the auxiliary information of ‘00000001,’ ‘00,’ ‘10’ and ‘01’.

### C. Data-Extraction and Image-Recovery

The process of data-Extraction and image-Recovery is the reverse process of the payload embedding. At the receiver end, the secret information must be extracted error-free from the marked encrypted image with only the data-hiding key  $k_d$ , and the original plaintext image must be restored losslessly with only the encryption key  $k_e$ . According to different permissions, the receiver can obtain the original plaintext image, secret information or both.

1) *Data-Extraction:* After obtaining the marked encrypted image, the receiver can extract the secret information. First, we remain the pixels in  $P_r$  unchanged and extract the parameters  $\alpha$  and  $\beta$  from  $P_s$ . Second, for the rest pixels, we check the labels of their  $\alpha$  or  $\beta$  bits in the reverse 8-bit binary sequences and classify them into sets  $P_e$  and  $P_n$ . Third, the payload can be extracted from the remaining  $(8 - \alpha)$ -bit of each pixel in  $P_e$ , then we get the encrypted secret information. Finally, the plaintext secret information can be obtained by decrypting using the data-hiding key  $k_d$ .

2) *Image-Recovery:* On the other hand, the replaced  $\beta$ -bit of each pixel in  $P_n$  and 8-bit of the pixel in  $P_s$  can be restored using the auxiliary information from the extracted payload. Then the original values of  $P_n$  and  $P_s$  must be obtained by decrypting using the encryption key  $k_e$ . Furthermore, the original value of  $P_r$  must be obtained by decrypting directly using the encryption key  $k_e$  as the pixels in  $P_r$  remain unchanged. So far, we restore all the pixels except for the pixels in  $P_e$ . For each pixel in  $P_e$ , according to its restored left, upper and upper left neighboring pixels, we obtain the corresponding prediction value  $px$  by Eq. (2), and according to its  $\alpha$ -bit labeling bits, we obtain the corresponding prediction error  $e$ . Then the original value  $x$  of each pixel in  $P_e$  can be obtained by the following Eq. (10). By now

$P_n$	$P_e$					
	2	1	0	$-1$	$-2$	$-3$
00	111	110	101	100	011	010
	111	110	101	100	011	010

(a)

00011011	11110110	11000110	10111101	11101011
11100000	00101101	10011110	00100100	00011001
11000000	10001001	10100110	00111100	00011110
10001111	10001110	11100001	11111000	00000001

(b)

00011011	11110110	11000110	10111101	11101011
11100000	10110100	01111001	00100100	10011000
11000000	10010001	01100101	00111100	01111000
10001111	01110001	10000111	00011111	00000001

(c)

00011011	11110110	11000110	10111101	11101011
11100000	11110100	10011001	00100100	00011000
11000000	01110001	10100101	11111100	01111000
10001111	00110001	10000111	10011111	00110010

(d)

00011011	11110110	11000110	10111101	11101011
11100000	00101111	10011001	00100100	00011000
11000000	10001110	10100101	00111111	00011110
10001111	10001100	11100001	11111001	00110010

(e)

00011011	11110110	11000110	10111101	11101011
11100000	-----111	-----001	00100100	00011000
11000000	-----110	-----101	-----111	-----110
10001111	10001100	-----001	-----001	00110010

(f)

Fig. 7. Illustrative example of pixel labeling and payload embedding when  $\alpha = 3$  and  $\beta = 2$ : (a) Labeling bits selection, (b) The 8-bit binary representation of Fig. 5(d), (c) Reverse order of 8-bit binary sequence in  $P_e$  and  $P_n$ , (d) Pixel bits after pixel labeling, (e) Encrypted image with labels and (f) Marked encrypted image.

the original content of the image is fully recovered.

$$x = px + e \quad (10)$$

Due to the reversibility of each step above, the proposed IPBTL-RDHEI method is separable and error-free in data-extraction and image-recovery.

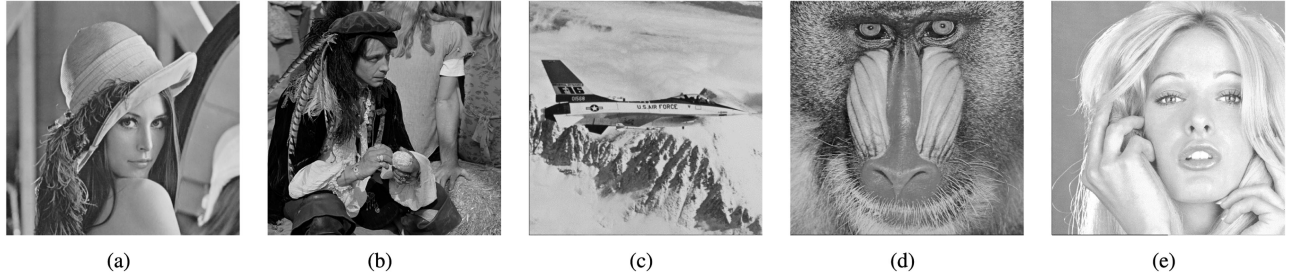
Fig. 8. Test images: (a) *Lena*, (b) *Man*, (c) *Jetplane*, (d) *Baboon*, and (e) *Tiffany*.

TABLE III  
EMBEDDING RATE  $r_{\alpha,\beta}$  (BPP) OF TEST IMAGES WHEN  $\beta = 2$  AND  $\alpha = 1$  TO 7

$(\alpha,\beta)$	(1,2)	(2,2)	(3,2)	(4,2)	(5,2)	(6,2)	(7,2)
Lena	/	0.3933	1.6609	2.6867	2.6447	1.9285	0.9919
Man	/	/	0.8173	2.0024	2.4790	1.9094	0.9894
Jetplane	/	1.5395	2.6098	3.0250	2.6726	1.9223	0.9925
Baboon	/	/	/	0.2039	0.9692	1.2402	0.8615
Tiffany	/	0.7108	1.9811	2.8478	2.6515	1.9288	0.9928

TABLE IV  
EMBEDDING RATE  $r_{\alpha,\beta}$  (BPP) OF TEST IMAGES WHEN  $\beta = 3$  AND  $\alpha = 1$  TO 7

$(\alpha,\beta)$	(1,3)	(2,3)	(3,3)	(4,3)	(5,3)	(6,3)	(7,3)
Lena	/	/	1.7087	2.7872	2.6770	1.9407	0.9929
Man	/	/	0.6546	2.0924	2.5517	1.9925	0.9915
Jetplane	/	0.9849	2.6962	3.0589	2.6900	1.9347	0.9939
Baboon	/	/	/	/	0.8789	1.2502	0.8896
Tiffany	/	0.0525	2.0743	2.9204	2.6793	1.9416	0.9946

TABLE V  
EMBEDDING RATE  $r_{\alpha,\beta}$  (BPP) OF TEST IMAGES WHEN  $\beta = 4$  AND  $\alpha = 1$  TO 7

$(\alpha,\beta)$	(1,4)	(2,4)	(3,4)	(4,4)	(5,4)	(6,4)	(7,4)
Lena	/	/	1.2997	2.7703	2.6693	1.9423	0.9933
Man	/	/	0.1126	2.0374	2.5516	1.9226	0.9919
Jetplane	/	0.4303	2.4107	3.0266	2.6778	1.9360	0.9942
Baboon	/	/	/	/	0.6866	1.2002	0.8953
Tiffany	/	/	1.7111	2.8941	2.6703	1.9436	0.9949

#### IV. EXPERIMENTAL RESULTS AND ANALYSIS

Several experiments are performed to evaluate the performance of the proposed IPBTL-RDHEI method. Five common 8-bit depth images are used, as shown in Fig. 8. Moreover, in order to reduce the influence caused by the random selection of test images, three datasets including UCID [22], BOSSBase [23], and BOWS-2 [24] are also tested respectively. We use two metrics with PSNR (peak signal-to-noise ratio) and SSIM (structural similarity) to evaluate the similarity between two images. The embedding rate (ER) is expressed in bpp and is the key indicator, which is expected to be as large as possible.

#### A. Performance and Security Analysis

In this section, we evaluate the performance of the proposed IPBTL-RDHEI method on the test images separately. Tables III–V show the maximal embedding rates of test images when  $\beta = 2$  to 4 and  $\alpha = 1$  to 7. We can see when  $\alpha$  is small, such as  $\alpha = 1$  or 2, the proposed IPBTL-RDHEI method cannot or can only embed a small amount of secret information. The ‘/’ in Tables III–V indicates that the auxiliary information is larger than the reserved room, thus no secret information can be embedded. From Tables III–V, we also can observe that different parameter settings should be selected for different images to

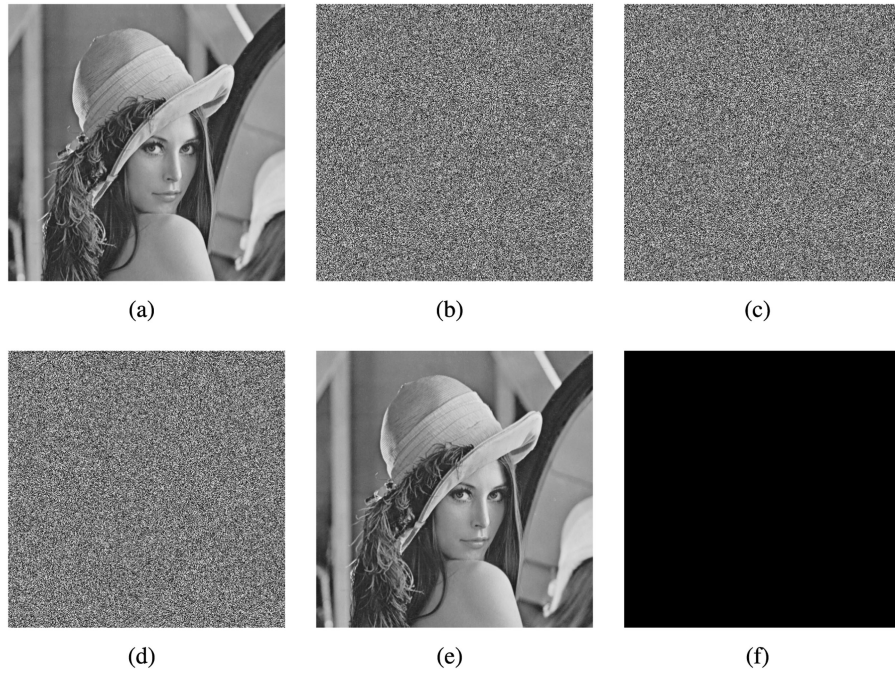


Fig. 9. Simulation results of applying the proposed IPBTL-RDHEI method to *Lena* image when  $\alpha = 5$  and  $\beta = 2$ : (a) original image, (b) encrypted image, (c) encrypted image with labels, (d) marked encrypted image,  $r_{\max} = 2.6447$  bpp, (e) recovered image,  $PSNR \rightarrow +\infty$  and  $SSIM = 1$ , (f) the difference between (a) and (e)

TABLE VI  
ENCRYPTED IMAGES' PSNR AND SSIM WITH THE ORIGINAL IMAGES WHEN  
 $\alpha = 5$  AND  $\beta = 2$

Encrypted image	Lena	Man	Jetplane	Baboon	Tiffany
PSNR (dB)	9.2255	7.9937	8.0077	9.5108	6.8839
SSIM	0.0341	0.0681	0.0346	0.0299	0.0389

reach the maximal embedding rate. In addition, the effect of image texture complexity on embedding rate is significant. A relatively smooth image has a higher embedding rate because there are more pixels belonging to  $P_e$ . For example, image *Jetplane* can achieve the maximal embedding rate of 3.0589 bpp when  $\alpha = 4$  and  $\beta = 3$ .

Fig. 9 takes *Lena* as an example to show different images in different phases generated by the proposed IPBTL-RDHEI method. Fig. 9(a) is the original image. Fig. 9(b) shows the encrypted image obtained by an encryption key  $k_e$ . The encrypted image with labels is shown in Fig. 9(c). Fig. 9(d) presents the marked encrypted image. Fig. 9(e) gives the recovered image, which is the same as Fig. 9(a). Fig. 9(f) is the difference between Fig. 9(a) and Fig. 9(e), where all pixels are 0. Fig. 9(b), (c) and (d) are three encrypted versions of Fig. 9(a), and it is difficult to detect the content of Fig. 9(a) from Fig. 9(b), (c) and (d), which means that the proposed IPBTL-RDHEI method has a high perceptual security level.

To further test the security of our method, Tables VI–VIII show the PSNR and SSIM values for each encrypted version image with the corresponding original image. From Tables VI–VIII, we can see that the PSNR value of each encrypted version

TABLE VII  
ENCRYPTED IMAGES WITH LABELS' PSNR AND SSIM WITH THE ORIGINAL  
IMAGES WHEN  $\alpha = 5$  AND  $\beta = 2$

Encrypted image with labels	Lena	Man	Jetplane	Baboon	Tiffany
PSNR (dB)	9.2256	8.0096	7.9935	9.5215	6.8741
SSIM	0.0347	0.0695	0.0353	0.0306	0.0391

TABLE VIII  
MARKED ENCRYPTED IMAGES' PSNR AND SSIM WITH THE ORIGINAL  
IMAGES WHEN  $\alpha = 5$  AND  $\beta = 2$

Marked encrypted image	Lena	Man	Jetplane	Baboon	Tiffany
PSNR (dB)	9.2222	8.0176	7.9941	9.5182	6.8838
SSIM	0.0351	0.0694	0.0359	0.0325	0.0375

image is very low and the SSIM value of each encrypted version image is almost 0. Thus no information can be obtained from these encrypted version images, which means that the proposed IPBTL-RDHEI method securely protects the privacy of the original image and can be applied to the RDH in the encryption domain.

#### B. Comparisons With Related Methods and Analysis

In this section, we compare the embedding rate of the proposed IPBTL-RDHEI method with several state-of-the-art methods. The parameters  $\alpha$  and  $\beta$  in the proposed IPBTL-RDHEI

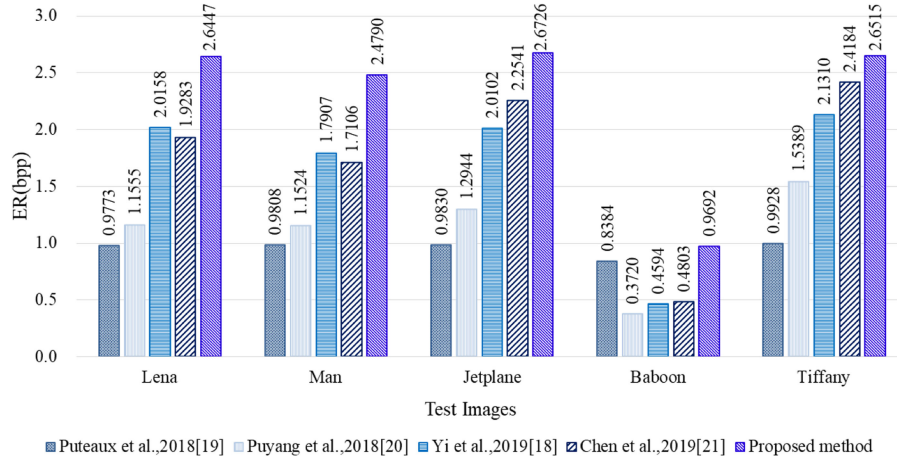


Fig. 10. Comparison of maximal embedding rates of test images between our method and four state-of-the-art methods.

TABLE IX  
DETAILED EMBEDDING RATES OF OUR METHOD ON THE THREE DATASETS WHEN  $\alpha = 5$  AND  $\beta = 2$

Datasets	Indicators	Best case	Worst case	Average
UCID	ER (bpp)	2.9759	0	2.2683
	PSNR (dB)	$+\infty$	$+\infty$	$+\infty$
	SSIM	1	1	1
BOSSbase	ER (bpp)	2.9883	0.0713	2.5613
	PSNR (dB)	$+\infty$	$+\infty$	$+\infty$
	SSIM	1	1	1
BOWS-2	ER (bpp)	2.9883	0.0484	2.5194
	PSNR (dB)	$+\infty$	$+\infty$	$+\infty$
	SSIM	1	1	1

method are set to 5 and 2. To obtain a better performance, we set the length of fixed-length codewords to 3 and block size to  $4 \times 4$  in [21]. In [18], the parameters  $\alpha$  and  $\beta$  are also set to 5 and 2, and the block size is set to  $3 \times 3$ .

Fig. 10 shows the maximal embedding rates of test images, compared with four competitors [18], [19], [20] and [21]. We can see that the proposed IPBTL-RDHEI method achieves higher embedding rate and outperforms the competitors.

Moreover, in order to reduce the influence caused by the random selection of test images, the detailed embedding rates of the proposed IPBTL-RDHEI method on the three datasets are shown in Table IX. For the best cases, the embedding rates are 2.9759 bpp, 2.9883 bpp, and 2.9883 bpp, respectively. Since  $\alpha$  is set to 5, that is, each pixel in  $P_e$  is labeled with 5 bits, and the remaining 3 bits can be embedded payload bits by bit replacement, thus the embedding rates approach 3 bpp in the best cases. In the UCID dataset, the worst embedding rate is 0 bpp, which means that the auxiliary information is larger than the reserved room, therefore no secret information is embedded when  $\alpha = 5$  and  $\beta = 2$ . Also, Table IX indicates that each

original plaintext image can be recovered error-free ( $PSNR \rightarrow +\infty$  and  $SSIM = 1$ ).

Fig. 11 compares the average embedding rates of the three datasets between the proposed IPBTL-RDHEI method and these four state-of-the-art methods. The average embedding rates on the three datasets are close to 1 bpp but no more than 1 bpp in the EPE-HCRDH method [19]. The method of two-MSB planes substitution in [20] has higher embedding rate than EPE-HCRDH [19]. In addition, the average embedding rates of Chen *et al.*'s method [21] are higher, reaching 1.8768 bpp in the UCID dataset, 2.3226 bpp in the BOSSBase dataset and 2.2447 bpp in the BOWS-2 dataset, respectively. Both Yi *et al.*'s method [18] and our method are based on PBTL. The results in Fig. 11 show that the proposed IPBTL-RDHEI method significantly improves the embedding rate compared with Yi *et al.*'s method [18]. There are two main reasons for this: first, the proposed IPBTL-RDHEI method reserves room in the plaintext image before encryption, which can take full advantage of the image redundancy; second, we take advantage of the spatial correlation in the entire original image but not in small image blocks

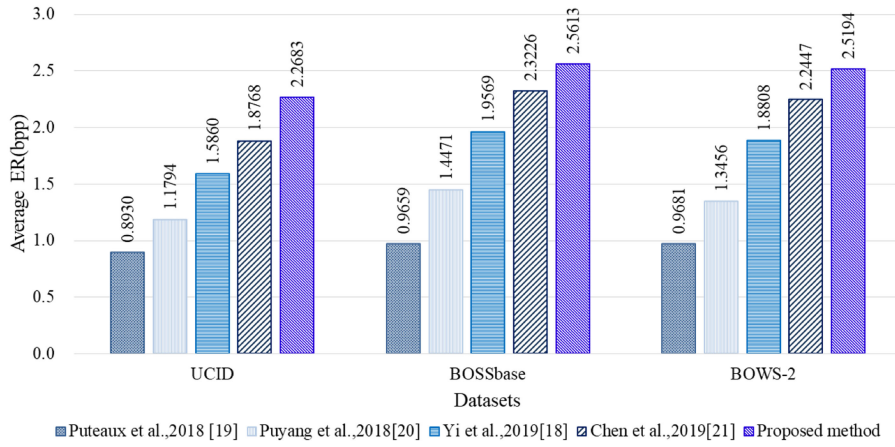


Fig. 11. Comparison of the average embedding rates of three datasets between our method and four state-of-the-art methods.

to reserve room for embedding data, which reduces the number of  $P_r$ , that results in less auxiliary information. Based on the above analysis, we can see that the proposed IPBTL-RDHEI method has better performance.

## V. CONCLUSION

This paper presents an effective method of RDH in the encryption domain using parametric binary tree labeling, which is an improved method based on Yi *et al.*'s work [18]. The proposed IPBTL-RDHEI method provides a good level of security that can be applied to protect the privacy of the original plaintext image. In addition, compared with the state-of-the-art methods, the proposed IPBTL-RDHEI method takes full advantage of the image redundancy, which not only is separable and error-free in image-recovery and data-extraction but also achieves higher embedding rate. In further research, we will test other error predictors to make more pixels into the embeddable pixel set, then more pixels can be utilized to embed secret information.

## REFERENCES

- [1] P. Tsai, Y. Hu, and H. L. Yeh, "Reversible image hiding scheme using predictive coding and histogram shifting," *Signal Process.*, vol. 89, no. 6, pp. 1129–1143, 2009.
- [2] X. Chen, X. Sun, H. Sun, Z. Zhou, and J. Zhang, "Reversible watermarking method based on asymmetric-histogram shifting of prediction errors," *J. Syst. Softw.*, vol. 86, no. 10, pp. 2620–2626, 2013.
- [3] X. Zhang, "Reversible data hiding with optimal value transfer," *IEEE Trans. Multimedia*, vol. 15, no. 2, pp. 316–325, Feb. 2013.
- [4] X. Li, W. Zhang, X. Gui, and B. Yang, "Efficient reversible data hiding based on multiple histograms modification," *IEEE Trans. Inf. Forensics Secur.*, vol. 10, no. 9, pp. 2016–2027, Sep. 2015.
- [5] J. Fridrich, M. Goljan, and R. Du, "Lossless data embedding: New paradigm in digital watermarking," *EURASIP J. Appl. Signal Process.*, vol. 2002, no. 2, pp. 185–196, 2002.
- [6] M. U. Celik, G. Sharma, A. M. Tekalp, and E. Saber, "Lossless generalized-LSB data embedding," *IEEE Trans. Image Process.*, vol. 14, no. 2, pp. 253–266, Feb. 2005.
- [7] A. M. Alattar, "Reversible watermark using the difference expansion of a generalized integer transform," *IEEE Trans. Image Process.*, vol. 13, no. 8, pp. 1147–1156, Aug. 2004.
- [8] D. M. Thodi and J. J. Rodriguez, "Expansion embedding techniques for reversible watermarking," *IEEE Trans. Image Process.*, vol. 16, no. 3, pp. 721–730, Mar. 2007.
- [9] V. Sachnev, H. J. Kim, J. Nam, S. Suresh, and Y. Shi, "Reversible watermarking algorithm using sorting and prediction," *IEEE Trans. Circuits Syst. Video Technol.*, vol. 19, no. 7, pp. 989–999, Jul. 2009.
- [10] L. Luo, Z. Chen, M. Chen, X. Zeng, and Z. Xiong, "Reversible image watermarking using interpolation technique," *IEEE Trans. Inf. Forensics Secur.*, vol. 5, no. 1, pp. 187–193, Mar. 2010.
- [11] X. Li, W. Zhang, X. Gui, and B. Yang, "A novel reversible data hiding scheme based on two-dimensional difference-histogram modification," *IEEE Trans. Inf. Forensics Secur.*, vol. 8, no. 7, pp. 1091–1100, Jul. 2013.
- [12] W. Puech, M. Chaumont, and O. Strauss, "A reversible data hiding method for encrypted images," in *Proc. Secur., Forensics, Steganography, Watermarking Multimedia Contents X*, vol. 6819. Bellingham, WA, USA: SPIE, 2008, p. 68191E.
- [13] J. Zhou *et al.*, "Secure reversible image data hiding over encrypted domain via key modulation," *IEEE Trans. Circuits Syst. Video Technol.*, vol. 26, no. 3, pp. 441–452, Mar. 2016.
- [14] Z. Qian, X. Zhang, and S. Wang, "Reversible data hiding in encrypted jpeg bitstream," *IEEE Trans. Multimedia*, vol. 16, no. 5, pp. 1486–1491, Aug. 2014.
- [15] K. Ma, W. Zhang, X. Zhao, N. Yu, and F. Li, "Reversible data hiding in encrypted images by reserving room before encryption," *IEEE Trans. Inf. Forensics Secur.*, vol. 8, no. 3, pp. 553–562, Mar. 2013.
- [16] X. Liao, K. Li, and J. Yin, "Separable data hiding in encrypted image based on compressive sensing and discrete Fourier transform," *Multimedia Tools Appl.*, vol. 76, no. 20, pp. 20739–20753, 2017.
- [17] X. Zhang, "Separable reversible data hiding in encrypted image," *IEEE Trans. Inf. Forensics Secur.*, vol. 7, no. 2, pp. 826–832, Apr. 2012.
- [18] S. Yi and Y. Zhou, "Separable and reversible data hiding in encrypted images using parametric binary tree labeling," *IEEE Trans. Multimedia*, vol. 21, no. 1, pp. 51–64, Jan. 2019.
- [19] P. Pueaux and W. Puech, "An efficient MSB prediction-based method for high-capacity reversible data hiding in encrypted images," *IEEE Trans. Inf. Forensics Secur.*, vol. 13, no. 7, pp. 1670–1681, Jul. 2018.
- [20] Y. Puyang, Z. Yin, and Z. Qian, "Reversible data hiding in encrypted images with two-MSB prediction," in *Proc. IEEE Int. Workshop Inf. Forensics Secur.*, 2018, pp. 1–7.
- [21] K. Chen and C. Chang, "High-capacity reversible data hiding in encrypted images based on extended run-length coding and block-based MSB plane rearrangement," *J. Visual Commun. Image Representation*, vol. 58, no. 2019, pp. 334–344, 2019.
- [22] G. Schaefer and M. Stich, "UCID: An uncompressed color image database," in *Proc. Storage Retrieval Methods Appl. Multimedia*, vol. 5307. Bellingham, WA, USA: SPIE, 2003, pp. 472–481.
- [23] P. Bas, T. Filler, and T. Pevný, "Break our steganographic system: The ins and outs of organizing boss," in *Proc. Int. Workshop Inf. Hiding*, 2011, pp. 59–70.
- [24] P. Bas and T. Furon, "Image database of bows-2," 2017. [Online]. Available: <http://bows2.ec-lille.fr/>



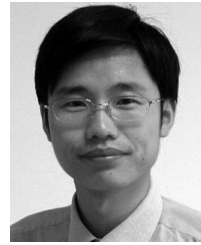
**Youqing Wu** received the B.E. and M.E. degrees in computer science and technology from Anhui University in 2006 and 2009, respectively. She is currently working with the School of Computer Science and Technology, Hefei Normal University. Her research interests include information hiding and multimedia security.



**Youzhi Xiang** received the bachelor's degree in computer science and technology in 2017 and now is a Master Student with the School of Computer Science and Technology, Anhui University. His current research interests include reversible data hiding in encrypted images.



**Yutang Guo** received the B.Eng., M.Eng., and Ph.D. degrees from Anhui University in 1987, 1990, and 2009, respectively. He is currently a Full Professor and a Master's Tutor with the School of Computer Science and Technology, Hefei Normal University. His research interests include image processing and pattern recognition.



**Jin Tang** received the B.Eng. degree in automation in 1999 and the Ph.D. degree in computer science in 2007 from Anhui University, Hefei, China. Since 2009, he has been a Professor with the School of Computer Science and Technology, Anhui University. His research interests include image processing, pattern recognition, machine learning, and computer vision.



**Zhaoxia Yin** received the B.Sc., M.E., and Ph.D. degrees from Anhui University in 2005, 2010, and 2014, respectively. She is an ACM/CCF Member, CSIG Senior Member, and was the Associate Chair of the academic committee of CCF YOCSEF Hefei from 2016 to 2017. She is currently working as an Associate Professor and a Ph.D. Advisor with the School of Computer Science and Technology, Anhui University. She is also the Principal Investigator of two NSFC Projects. Her primary research focus includes information hiding, multimedia security. She has published many SCI/EI indexed papers in journals, edited books, and refereed conferences.